Available online at www.sciencedirect.com
SCIENCE DIRECT®
Journal of Sound and Vibration 261 (2003) 927–944
JOURNAL OF SOUND AND VIBRATION
www.elsevier.com/locate/jsvi

An efficient coupled layerwise theory for dynamic analysis of piezoelectric composite beams

S. Kapuria, P.C. Dumir*, A. Ahmed

Applied Mechanics Department, Hauz khas, I.I.T. Delhi, New Delhi 110016, India

Received 22 January 2002; accepted 17 June 2002

Abstract

An efficient new coupled one-dimensional model is developed for the dynamics of piezoelectric composite beams. The model combines third order zigzag approximation for the displacement with layerwise approximation of the electric field as piecewise linear for sublayers. By enforcing the conditions of zero transverse shear stress at the top and bottom and its continuity at layer interfaces, the displacement field is expressed in terms of three primary displacement variables and potentials. The governing coupled equations of stress and charge equilibrium and boundary conditions are derived from Hamilton's principle. Analytical solutions are obtained, for free vibrations and forced response under harmonic load, for simply supported hybrid beams and the results are compared with the exact three-dimensional solution and uncoupled first order shear deformation theory solution. The present results show significant improvement over the first order solution and agree very well with the exact solution for both thin and thick hybrid beams. The results demonstrate the capability of the developed theory to adequately model open and closed circuit electric boundary conditions to accurately predict their influence on the response.

1. Introduction

Piezoelectric composite laminates with embedded or surface bonded piezoelectric layers form part of new generation of adaptive structures. The sensing and actuation capability of piezoelectric layers is used for achieving active vibration control, shape control, noise control, damage identification and compensation (health monitoring), etc. To realize these objectives, a robust electromechanical model is required which accounts for the electromechanical inhomogeneities in these hybrid laminates and provides accurate prediction of the sensory and

*Corresponding author. Tel.: +91-11-6591225; fax: +91-11-6581119.
E-mail address: pcd@am.iitd.ernet.in (P.C. Dumir).

0022-460X/03/$ - see front matter
PII: S0022-460X(02)01026-X

active response of the structure. A review of three-dimensional (3-D) continuum-based approaches, 2-D theories for plates and shells and 1-D theories for beams, along with their comparative study for plates under static loading, has been presented by Saravanos and Heyliger [1]. Analytical 3-D solutions are available only for some specific shapes with specific boundary conditions such as simply supported infinite flat panels [2] and rectangular plates [3,4]. On the other hand, a 3-D finite element analysis [5] results in large problem size which may become computationally intractable for practical dynamics and control problems. Hence there is need for accurate 2-D plate and 1-D beam theories and several theories of varying accuracy have been developed. Early works in adaptive structures employed induced strain models in which elastic beam models were employed [6–8] along with effective forces and moments due to induced strain of piezoelectric actuators. A discrete layer theory based on layerwise approximations for displacements was developed for elastic laminated beams with induced actuation strain by Robins and Reddy [9]. Classical laminate theory (CLT) approximation for the mechanical field has been applied by some researchers [10–12] without considering any electromechanical coupling. Later the transverse shear deformation effect was incorporated by using the first order shear deformation theory (FSDT) [13] and the refined third order theory [14–16] for the dynamics of hybrid beams and plates. Huang and Wu [17] and Huang and Sun [18] presented coupled FSDT solution for piezoelectric composite plates and beams including the charge equation of electrostatics and considering the electromechanical coupling. Mitchell and Reddy [19] presented a coupled hybrid theory for the dynamics of piezoelectric composite plates based on the third order approximation for the displacement field and layerwise approximation for the potential field. Zhou et al. [20] have developed coupled thermo-electromechanical theory to model dynamic response of hybrid plates using third order approximation for displacement and temperature fields and layerwise linear approximation for the potential field. Saravanos and Heyliger [21,22] have presented coupled discrete layer theories (DLT) based on layerwise approximation for displacement and potential fields and shown that these yield very accurate results for both thin and thick laminates. But these are expensive for practical problems since the number of unknowns depend on the number of layers. To overcome this disadvantage, Kapuria [23] has recently developed a novel coupled layerwise theory, for static analysis of piezoelectric composite beams, which combines a third order zig-zag approximation for the inplane displacement [24,25] with a sublayerwise piecewise linear approximation for the electric potential. The transverse displacement is approximated to account for the piezoelectric transverse normal strain induced by the electric potential. The conditions of zero shear stress conditions at the top and bottom surfaces and the conditions of transverse shear stress continuity at layer interfaces are enforced to formulate the theory in terms of only three displacement unknowns, which are independent of the number of layers and equal in number to the ones used in the FSDT. This layerwise theory for displacement and potential fields thus preserves the computational advantage of an equivalent single layer (ESL) theory and yet yields important through-the-thickness variations of displacements, electric field, inplane stresses and transverse shear stress. For simply supported hybrid beam under electro-mechanical load, this theory has yielded highly accurate results (by comparison with the exact 3-D solution) at global and local laminate level, which are superior to those of FSDT which uses the same number of displacement unknowns.

Encouraged by its excellent performance in the static case, this theory is extended to dynamics in the present paper. The coupled equations of stress and charge equilibrium and variationally

consistent boundary conditions for the developed model are derived using Hamilton's principle. The accuracy of the theory in estimating local and global response is assessed by comparison of an analytical solution, for the free and forced vibration of a simply supported hybrid beam, with the exact 3-D piezoelastic solution and uncoupled FSDT solution. The effects of ratio of span-to-thickness and ratio of piezolayer thickness to beam thickness on the response are investigated. The influence of electric boundary conditions applied in sensory and actuation applications on the free vibration response is studied to establish the effect of piezoelectric coupling.

2. Formulation of layerwise theory for dynamics

Consider a hybrid beam of width b, thickness h and length a, made of L perfectly bonded orthotropic layers with one of the principal material axes of each along the longitudinal axis x. Some of the layers can be of piezoelectric material with poling along the thickness axis z. The sensors and actuators, considered herein, are of orthorhombic materials of class mm2 symmetry [26], since the commonly used materials PZT and PVDF belong to this class. The material of the piezoelectric layers can be different. The midplane of the beam is chosen as the xy-plane. The z-coordinate of the bottom surface of the kth layer (numbered from the bottom) is denoted as z_{k-1}. For a beam with small width, assume plane state of stress ($\sigma_y = \tau_{yz} = \tau_{xy} = 0$), neglect transverse normal stress ($\sigma_z \simeq 0$) and assume the axial and transverse displacements u, w and electric potential ϕ to be independent of y ($\Rightarrow$ electric field component $E_y = -\phi_{,y} = 0$). The strain–displacement and electric field–potential relations for directions x, z are:

$$\varepsilon_x = u_{,x}, \quad \varepsilon_z = w_{,z}, \quad \gamma_{zx} = u_{,z} + w_{,x}; \quad E_x = -\phi_{,x}, \quad E_z = -\phi_{,z}, \tag{1}$$

where a subscript comma denotes differentiation. Unlike most other studies, E_x is not considered as zero, since it is an electric field induced by the piezoelectric coupling. With these assumptions, the general 3-D constitutive equations for stresses and electric displacements D_x, D_z reduce to [23]

$$\begin{aligned} &\sigma_x = Q_{11}\varepsilon_x - e_{31}E_z = Q_{11}u_{,x} + e_{31}\phi_{,z}, \quad \tau_{zx} = Q_{55}\gamma_{zx} - e_{15}E_x = Q_{55}(u_{,z} + w_{,x}) + e_{15}\phi_{,x}, \\ &D_x = e_{15}\gamma_{zx} + \eta_{11}E_x = e_{15}(u_{,z} + w_{,x}) - \eta_{11}\phi_{,x}, \quad D_z = e_{31}\varepsilon_x + \eta_{33}E_z = e_{31}u_{,x} - \eta_{33}\phi_{,z}, \end{aligned} \tag{2}$$

where $Q_{11} = Y_x, Q_{55} = G_{zx}, e_{31} = d_{31}Q_{11}, e_{15} = d_{15}Q_{55}, \eta_{11} = \varepsilon_{11} - d_{15}e_{15}, \eta_{33} = \varepsilon_{33} - d_{31}e_{31}$ with Young's modulus Y_x, shear modulus G_{zx}, piezoelectric strain constants d_{ij} and dielectric constants ε_{ij}.

The potential field is assumed as piecewise linear between N points z_j across the thickness h [23]:

$$\phi(x, z, t) = \sum_{j=1}^{N} \Psi^j(z)\phi^j(x, t), \tag{3}$$

where $\phi^j(x, t) = \phi(x, z^j, t)$ and $\Psi^j(z)$ are linear interpolation functions. N can be chosen independent of the number of layers L and is determined by the required accuracy of the electric field. Deflection w is approximated by integrating the constitutive equation for strain ε_z: $\varepsilon_z = -\nu_{xz}\sigma_x/E_x + d_{33}E_z \simeq d_{33}E_z$, by neglecting the contribution of the first term as in elastic

beam theory, to yield

$$w(x,z,t) = w_0(x,t) - \sum_{j=1}^{N} \bar{\Psi}^j(z)\phi^j(x,t), \tag{4}$$

where $\bar{\Psi}^j(z) = \int_0^z d_{33}\Psi^j_{,z}(z)\,\mathrm{d}z$ is a piecewise linear function. The formulation in Ref. [23] is applicable only if the hybrid beam has piezoelectric layers of the same material. For such a special case d_{33} is constant and the present Eq. (4) for the more general case, reduces to $w = w_0(x,t) - d_{33}\sum_{j=1}^{N}\Psi^j(z)\phi^j(x,t)$, which is same as Eq. (5b) of Ref. [23]. The longitudinal displacement is assumed [23], as in discrete layer elastic theory [24] to be a combination of a third order variation across the thickness with layerwise linear variation with slope discontinuities at the layer interfaces and an additional explicit layerwise contribution $g_k(x,z,t)$ due to electric potential ϕ. For the kth layer, u is assumed as

$$u(x,z,t) = z^2\xi(x,t) + z^3\eta(x,t) + u_k(x,t) + z\psi^*_k(x,t) + g_k(x,z,t). \tag{5}$$

u_k and ψ^*_k denote translation and rotation variables of the kth layer. Using Eqs. (2), (4) and (5) yields

$$\tau_{zx} = Q^k_{55}(2z\xi + 3z^2\eta + \psi^*_k + w_{0,x}) + \left[Q^k_{55}g_{k,z} - \sum_{j=1}^{N}(Q^k_{55}\bar{\Psi}^j - e^k_{15}\Psi^j)\phi^j_{,x}\right]. \tag{6}$$

The square parentheses terms are the explicit contribution of electric potential and the round parentheses terms include its implicit contribution. Neglecting the explicit contribution of ϕ in τ_{zx} in the static case [23] has yielded very accurate global results even for thick beams. Hence to obtain simpler algebraic problem of imposing continuity of τ_{zx} at the layer interfaces, without loss of accuracy for the global response, the square parentheses terms in Eq. (6) are neglected to yield

$$g_k(x,z,t) = \sum_{j=1}^{N} G^j_k(z)\phi^j_{,x}, \quad \text{with} \quad G^j_k(z) = \int_{z_{k-1}}^{z}\left(\bar{\Psi}^j - \frac{e^k_{15}}{Q^k_{55}}\Psi^j\right)\mathrm{d}z. \tag{7}$$

Using Eq. (7) and denoting $\psi_k(x,t) = \psi^*_k + w_{0,x}$, Eqs. (5) and (6) yield

$$u(x,z,t) = u_k(x,t) - zw_{0,x}(x,t) + z\psi_k(x,t) + z^2\xi(x,t) + z^3\eta(x,t) + \sum_{j=1}^{N} G^j_k(z)\phi^j_{,x}, \tag{8}$$

$$\tau_{zx} = Q^k_{55}(\psi_k + 2z\xi + 3z^2\eta). \tag{9}$$

Let the midplane of the beam lie in the k_0th layer and denote its displacement $u_0(x,0,t) = u_0(x,t)$. The functions u_k, ψ_k, ξ, η are expressed as in Ref. [23] in terms of u_0 and ψ_1 using the $(k-1)$ conditions each for the continuity of τ_{zx} and u at the layer interfaces and the two shear traction-free conditions $\tau_{zx} = 0$ at $z = \pm h/2$. Thus

$$u = u_0 - zw_{0,x} + R_k(z)\psi_1 + \sum_{j=1}^{N} F^j_k(z)\phi^j_{,x}, \tag{10}$$

where

$$R_k(z) = R^k_1 + zR^k_2 + z^2R_3 + z^3R_4, \quad F^j_k(z) = G^j_k(z) + R^{kj}_0,$$

with

$$R_0^{kj} = \sum_{i=2}^{k} [G_{i-1}^j(z_{i-1}) - G_i^j(z_{i-1})] - \sum_{i=2}^{k_0} [G_{i-1}^j(z_{i-1}) - G_i^j(z_{i-1})], \tag{11}$$

$$R_4 = -4C_1^L/3h(hC_1^L + 4C_2^L),\ \ R_3 = 4C_2^L/h(hC_1^L + 4C_2^L),$$

$$R_2^k = 2(C_1^k/\bar{Q}_{55}^k - z_k)R_3 + 3(2C_2^k/\bar{Q}_{55}^k - z_k^2)R_4,$$

$$R_1^k = \sum_{i=2}^{k} z_{i-1}(R_2^{i-1} - R_2^i) - \sum_{i=2}^{k_0} z_{i-1}(R_2^{i-1} - R_2^i),\ \ C_1^k = \sum_{i=1}^{k} Q_{55}^i(z_i - z_{i-1}),$$

$$C_2^k = \sum_{i=1}^{k} Q_{55}^i(z_i^2 - z_{i-1}^2)/2.$$

The number of the primary variables is thus the same as in the first order shear deformation theory. The layerwise approximation of the electric potential enables effective modelling of the heterogeneity in the electric field across the thickness, induced by piezoelectric sensor and actuator layers.

The dynamic field equations and the variationally consistent boundary conditions have been formulated using Hamilton's principle for a piezoelectric continuum [27]:

$$\int_{t_1}^{t_2} \left[\int_V (\rho \dot{u}_i \delta \dot{u}_i - \sigma_{ij} \delta \varepsilon_{ij} - D_i \delta E_i)\, \mathrm{d}V + \int_A (T_i^n u_i - q\phi)\, \mathrm{d}A \right] \mathrm{d}t = 0,$$

with $(\delta u_i, \delta\phi) = 0$ at times $t = t_1, t_2$. V and A are the volume and surface of the body. T_i^n are the surface tractions and q is the surface charge density. The details of the derivation are omitted for brevity. Let ρ be the mass density and the overdot represents differentiation with respect to time. The equations of motion for u_0, w_0, ψ_1 and dynamic equations for electric potentials ϕ^j are:

$$-I_1\ddot{u}_0 + I_2\ddot{w}_{0,x} - I_3\ddot{\psi}_1 - \sum_{l=1}^{N} I_4^l \ddot{\phi}_{,x}^l + N_{x,x} = 0,$$

$$-I_2\ddot{u}_{0,x} + I_5\ddot{w}_{0,xx} - I_6\ddot{\psi}_{1,x} - I_1\ddot{w}_0 - \sum_{l=1}^{N}(I_7^l\ddot{\phi}_{,xx}^l - I_{11}^l\ddot{\phi}_{,x}^l) + M_{x,xx} + f_z = 0,$$

$$-I_3\ddot{u}_0 + I_6\ddot{w}_{0,x} - I_8\ddot{\psi}_1 - \sum_{l=1}^{N} I_9^l \ddot{\phi}_{,x}^l + P_{x,x} - Q_x = 0,$$

$$I_4^j\ddot{u}_{0,x} - I_7^j\ddot{w}_{0,xx} + I_9^j\ddot{\psi}_{1,x} + I_{11}\ddot{w}_0 + \sum_{l=1}^{N}(I_{10}^{jl}\ddot{\phi}_{,xx}^l - I_{12}^{jl}\ddot{\phi}^l) + H_{,x}^j$$

$$- G^j - S_{x,xx}^j - \bar{Q}_{x,x}^j + b[p_z^2\bar{\Psi}^j(z_L) - p_z^1\bar{\Psi}^j(z_0) - q^j] = 0 \quad (j = 1, 2, \ldots, N), \tag{12}$$

where $z_0 = -h/2,\ z_L = h/2$ and I_i, I_i^j and I_i^{jl} are the 12 inertia terms defined as

$$I_1 = \int_{-h/2}^{h/2} b\rho \,\mathrm{d}z, \quad I_2 = \int_{-h/2}^{h/2} b\rho z \,\mathrm{d}z, \quad I_3 = \sum_{k=1}^{L} \int_{z_{k-1}}^{z_k} b\rho R_k(z) \,\mathrm{d}z,$$

$$I_4^j = \sum_{k=1}^{L} \int_{z_{k-1}}^{z_k} b\rho F_k^j(z) \,\mathrm{d}z, \quad I_5 = \int_{-h/2}^{h/2} b\rho z^2 \,\mathrm{d}z, \quad I_6 = \sum_{k=1}^{L} \int_{z_{k-1}}^{z_k} b\rho z R_k(z) \,\mathrm{d}z,$$

$$I_7^j = \sum_{k=1}^{L} \int_{z_{k-1}}^{z_k} b\rho z F_k^j(z) \,\mathrm{d}z, \quad I_8 = \sum_{k=1}^{L} \int_{z_{k-1}}^{z_k} b\rho [R_k(z)]^2 \,\mathrm{d}z, \quad I_9^j = \sum_{k=1}^{L} \int_{z_{k-1}}^{z_k} b\rho R_k(z) F_k^j(z) \,\mathrm{d}z,$$

$$I_{10}^{jl} = \sum_{k=1}^{L} \int_{z_{k-1}}^{z_k} b\rho F_k^j(z) F_k^l(z) \,\mathrm{d}z, \quad I_{11}^j = \sum_{k=1}^{L} \int_{z_{k-1}}^{z_k} b\rho \bar{\Psi}^j(z) \,\mathrm{d}z,$$

$$I_{12}^{jl} = \sum_{k=1}^{L} \int_{z_{k-1}}^{z_k} b\rho \bar{\Psi}^j(z) \bar{\Psi}^l(z) \,\mathrm{d}z. \tag{13}$$

N_x, M_x, P_x, Q_x, S_x^j, $\bar{Q}_x^j$ are stress resultants and H^j, G^j are electric displacement resultants, defined as

$$N_x = \int_{-h/2}^{h/2} b\sigma_x \,\mathrm{d}z = A_{11} u_{0,x} - B_{11} w_{0,xx} + F_{11} \psi_{1,x} + \sum_{l=1}^{N} (\bar{F}_{11}^l \phi_{,xx}^l + \beta_1^l \phi^l),$$

$$M_x = \int_{-h/2}^{h/2} bz\sigma_x \,\mathrm{d}z = B_{11} u_{0,x} - D_{11} w_{0,xx} + E_{11} \psi_{1,x} + \sum_{l=1}^{N} (\bar{E}_{11}^l \phi_{,xx}^l + \beta_2^l \phi^l),$$

$$P_x = \sum_{k=1}^{L} \int_{z_{k-1}}^{z_k} bR_k(z)\sigma_x \,\mathrm{d}z = F_{11} u_{0,x} - E_{11} w_{0,xx} + G_{11} \psi_{1,x} + \sum_{l=1}^{N} (\bar{G}_{11}^l \phi_{,xx}^l + \beta_3^l \phi^l),$$

$$S_x^j = \sum_{k=1}^{L} \int_{z_{k-1}}^{z_k} bF_k^j(z)\sigma_x \,\mathrm{d}z = \bar{F}_{11}^j u_{0,x} - \bar{E}_{11}^j w_{0,xx} + \bar{G}_{11}^j \psi_{1,x} + \sum_{l=1}^{N} (\bar{H}_{11}^{jl} \phi_{,xx}^l + \beta_4^{jl} \phi^l),$$

$$Q_x = \sum_{k=1}^{L} \int_{z_{k-1}}^{z_k} bR_k(z)_{,z} \tau_{zx} \,\mathrm{d}z = D_{55} \psi_1, \quad \bar{Q}_x^j = \sum_{k=1}^{L} b(e_{15}^k / Q_{55}^k) \int_{z_{k-1}}^{z_k} \Psi^j(z) \tau_{zx} \,\mathrm{d}z = \bar{D}_{55}^j \psi_1,$$

$$H^j = \int_{-h/2}^{h/2} b\Psi^j(z) D_x \,\mathrm{d}z = \bar{D}_{55}^j \psi_1 - \sum_{l=1}^{N} \hat{E}_{11}^{jl} \phi_{,x}^l,$$

$$G^j = \int_{-h/2}^{h/2} b\Psi^j(z)_{,z} D_z \,\mathrm{d}z = \beta_1^j u_{0,x} - \beta_2^j w_{0,xx} + \beta_3^j \psi_{1,x} + \sum_{l=1}^{N} (\beta_4^{lj} \phi_{,xx}^l - \beta_5^{jl} \phi^l) \tag{14}$$

with

$$[A_{11}, B_{11}, D_{11}, F_{11}, E_{11}, G_{11}] = \int_{-h/2}^{h/2} b\, Q_{11}[1, z, z^2, R_k(z), zR_k(z), R_k^2(z)]\,\mathrm{d}z,$$

$$[\bar{F}_{11}^j, \bar{E}_{11}^j, \bar{G}_{11}^j, \bar{H}_{11}^{jl}] = \int_{-h/2}^{h/2} b\, Q_{11} F_k^j(z)[1, z, R_k(z), F_k^l(z)]\,\mathrm{d}z,$$

$$[\beta_1^l, \beta_2^l, \beta_3^l, \beta_4^{jl}] = \int_{-h/2}^{h/2} b\, e_{31}[1, z, R_k(z), F_k^j(z)]\Psi_{,z}^l(z)\,\mathrm{d}z, \quad \beta_5^{jl} = \int_{-h/2}^{h/2} b\,\eta_{33}\Psi_{,z}^j\Psi_{,z}^l\,\mathrm{d}z,$$

$$D_{55} = \int_{-h/2}^{h/2} bQ_{55}(R_{k,z})^2\,\mathrm{d}z, \quad \bar{D}_{55}^j = \int_{-h/2}^{h/2} be_{15}\Psi^j(z)R_{k,z}\,\mathrm{d}z,$$

$$\hat{E}^{jl} = \int_{-h/2}^{h/2} b\left[\eta_{11}^k + \frac{(e_{15}^k)^2}{Q_{55}^k}\right]\psi^j(z)\Psi^l(z)\,\mathrm{d}z. \tag{15}$$

The load $f_z = b(p_z^1 - p_z^2)$ where p_z^1 and p_z^2 are the normal pressures on the bottom and top surfaces of the beam and q^j are the surface charge densities at those locations of z^j where potential or charge density is prescribed. Hamilton's principle yields the following essential or natural boundary conditions at the ends of the beam at $x = 0, a$:

$$u_0 = u_0^* \quad \text{or} \quad N_x = N_x^*;$$

$$w_0 = w_0^* \quad \text{or} \quad -I_2\ddot{u}_0 + I_5\ddot{w}_{0,x} - I_6\ddot{\psi}_1 - \sum_{l=1}^{N} I_7^l\ddot{\phi}_{,x}^l + M_{x,x} = \left[\int_{-h/2}^{h/2} b\tau_{zx}\,\mathrm{d}z\right]^*;$$

$$w_{0,x} = w_{0,x}^* \quad \text{or} \quad M_x = M_x^*; \quad \psi_1 = \psi_1^* \quad \text{or} \quad P_x = P_x^*; \quad \phi_{,x}^j = \phi_x^{j*} \quad \text{or} \quad S_x^j = S_x^{j*};$$

$$\phi^j = \phi^{j*} \quad \text{or} \quad I_4^j\ddot{u}_0 - I_7^j\ddot{w}_{0,x} + I_9^j\ddot{\psi}_1 + \sum_{l=1}^{N} I_{10}^{jl}\ddot{\phi}_{,x}^l - S_{x,x}^j$$

$$-\bar{Q}_x^j + H^j = \bar{H}^{j*} + \left[\int_{-h/2}^{h/2} \tau_{zx}\bar{\Psi}^j\,\mathrm{d}z\right]^*; \tag{16}$$

where $*$ refers to prescribed value.

Substitution of the expressions from Eqs. (14) into Eqs. (12) yields the following dynamic equations for the primary field variables $(u_0, w_0, \psi_1, \phi^j)$:

$$-[\bar{L}_{ij}]\ddot{\bar{U}} + [L_{ij}]\bar{U} = P, \tag{17}$$

where $\bar{U} = [u_0\ w_0\ \psi_1\ \phi^1\ \phi^2\ \ldots\ \phi^N]^{\mathrm{T}}$, $P = [0\ f_z\ 0\ \bar{q}^1\ \bar{q}^2\ \ldots \bar{q}^N]^{\mathrm{T}}$ with $\bar{q}^l = b[q^l + p_z^1\bar{\Psi}^l(z_0) - p_z^2\bar{\Psi}^l(z_L)]$. $\bar{L}_{ij}$ and L_{ij} are linear differential operators with $\bar{L}_{ij} = \bar{L}_{ji}$, $L_{ij} = L_{ji}$ and

are given by

$$\bar{L}_{11} = I_1, \quad \bar{L}_{12} = -I_2(\ )_{,x}, \quad \bar{L}_{13} = I_3, \quad \bar{L}_{1,3+l} = I_4^l(\ )_{,x}, \quad \bar{L}_{22} = I_5(\ )_{,xx} - I_1,$$
$$\bar{L}_{23} = -I_6(\ )_{,x}, \quad \bar{L}_{2,3+l} = I_{11}^l - I_7^l(\ )_{,xx}, \quad \bar{L}_{33} = I_8, \quad \bar{L}_{3,3+l} = I_9^l(\ )_{,x},$$
$$\bar{L}_{3+m,3+l} = I_{10}^{ml}(\ )_{,xx} - I_{12}^{ml},$$
$$L_{11} = A_{11}(\ )_{,xx}, \quad L_{12} = -B_{11}(\ )_{,xxx}, \quad L_{13} = F_{11}(\ )_{,xx}, \quad L_{1,3+l} = \bar{F}_{11}^l(\ )_{,xxx} + \beta_1^l(\ )_{,x},$$
$$L_{22} = D_{11}(\ )_{,xxxx}, \quad L_{23} = -E_{11}(\ )_{,xxx}, \quad L_{2,3+l} = -\bar{E}_{11}^l(\ )_{,xxxx} - \beta_2^l(\ )_{,xx}, \quad L_{33} = G_{11}(\ )_{,xx} - D_{55},$$
$$L_{3,3+l} = \bar{G}_{11}^l(\ )_{,xxx} + \beta_3^l(\ )_{,x}, \quad L_{3+m,3+l} = \bar{H}_{11}^{ml}(\ )_{,xxxx} + (\beta_4^{ml} + \beta_4^{lm} + \hat{E}_{11}^{ml})(\ )_{,xx} - \beta_5^{ml},$$
$$(m,l) = 1, \ldots N. \tag{18}$$

After solving for U, τ_{zx} can be obtained using constitutive equation (2) directly or more accurately by integrating the 3-D equation of motion in x direction to yield $\tau_{zx} = \int_{-h/2}^{z}(\rho\ddot{u} - \sigma_{x,x})\,\mathrm{d}z$.

3. Analytical solution for simply supported beam

In order to assess the accuracy of the coupled zig-zag theory developed herein, an analytical solution is obtained for simply supported beams with the following boundary conditions at $x = 0, a$:

$$N_x = 0, \quad w_0 = 0, \quad M_x = 0, \quad P_x = 0, \quad \phi^j = 0, \quad S_x^j = 0, \qquad j = 1, \ldots, N \tag{19}$$

and compared with the exact piezoelastic solution [2]. The solution of Eq. (17) is expanded in Fourier series as

$$(w_0, \phi^j, N_x, M_x, P_x, S_x^j, G^j, f_z, \bar{q}^j) = \sum_{n=1}^{\infty} (w_0, \phi^j, N_x, M_x, P_x, S_x^j, G^j, f_z, \bar{q}^j)_n \sin \bar{n}x,$$
$$(u_0, \psi_1, Q_x, \bar{Q}_x^j, H^j) = \sum_{n=1}^{\infty} (u_0, \psi_1, Q_x, \bar{Q}_x^j, H^j)_n \cos \bar{n}x \tag{20}$$

with $\bar{n} = n\pi/a$. Substituting these in Eqs. (17) yields for nth Fourier component, the coupled equations

$$\begin{bmatrix} M^{uu} & M^{ue} \\ M^{eu} & M^{ee} \end{bmatrix} \begin{Bmatrix} \ddot{U}^n \\ \ddot{\Phi}^n \end{Bmatrix} + \begin{bmatrix} K^{uu} & K^{ue} \\ K^{eu} & K^{ee} \end{bmatrix} \begin{Bmatrix} U^n \\ \Phi^n \end{Bmatrix} = \begin{Bmatrix} F^n \\ Q^n \end{Bmatrix}, \tag{21}$$

where $U^n = [u_0 \ w_0 \ \psi_1]_n^{\mathrm{T}}$, $\Phi^n = [\bar{\phi}^1 \ \bar{\phi}^2 \ldots \bar{\phi}^N]_n^{\mathrm{T}}$, $F^n = [0 \ f_z \ 0]^{\mathrm{T}}$, $Q^n = [\bar{q}^1 \ \bar{q}^2 \ldots \bar{q}^N]_n^{\mathrm{T}}$ and M^{rs} and K^{rs} $(r = u, e; \ s = u, e)$ are submatrices of the symmetric inertia matrix M and stiffness matrix K.

Let $\Phi = [\Phi_s; \Phi_a]$, where Φ_s and Φ_a represent the sets of unknown voltages output and known active voltages input at the sensor and actuator layers. Eq. (21) can be partitioned and arranged as

$$\begin{bmatrix} M^{uu} & M_{ss}^{ue} \\ M_{ss}^{eu} & M_{ss}^{ee} \end{bmatrix} \begin{Bmatrix} \ddot{U}^n \\ \ddot{\Phi}_s^n \end{Bmatrix} + \begin{bmatrix} K^{uu} & K_{ss}^{ue} \\ K_{ss}^{eu} & K_{ss}^{ee} \end{bmatrix} \begin{Bmatrix} U^n \\ \Phi_s^n \end{Bmatrix} = \begin{Bmatrix} F^n - K_{sa}^{ue}\Phi_a^n - M_{sa}^{ue}\ddot{\Phi}_a^n \\ Q_s^n - K_{sa}^{ee}\Phi_a^n - M_{sa}^{ee}\ddot{\Phi}_a^n \end{Bmatrix}. \tag{22}$$

It can be solved for free and forced vibration response of the beam in active/sensory/active-sensory mode. For example, for synchronous free vibrations at natural frequency ω_n, let $\tilde{U}^n = [U^n \ \Phi_a^n]^{\mathrm{T}} = \tilde{U}_0^n \cos \omega_n t$ in Eq. (22) to yield the following generalized eigenvalue problem:

$$\left[\begin{bmatrix} K^{uu} & K_{ss}^{ue} \\ K_{ss}^{eu} & K_{ss}^{ee} \end{bmatrix} - \omega_n^2 \begin{bmatrix} M^{uu} & M_{ss}^{ue} \\ M_{ss}^{eu} & M_{ss}^{ee} \end{bmatrix}\right] \{\tilde{U}_0^n\} = \{0\}, \tag{23}$$

where $\tilde{U}_0^n$ are the through-the-thickness mode shapes for the given spatial mode n.

The exact piezoelastic solution for the simply supported hybrid beam is obtained, as in Ref. [2] for cylindrical bending of a panel by considering $\sigma_y = \tau_{yz} = \tau_{xy} = 0$, $E_y = 0$ but $\sigma_z \neq 0$ and with corresponding appropriate modification of the constants in the constitutive equations.

4. Numerical results and discussion

Consider simply supported hybrid beams made up of a substrate of graphite–epoxy composite with a piezoelectric layer of PZT-5A with thickness h_p bonded to its top, with properties the same as in Ref. [28]:

$$\begin{aligned} \text{composite}: &(Y_L, Y_T, G_{LT}, G_{TT}) = (181, 10.3, 7.17, 2.87)\ \text{GPa}, \ d_{ij} = 0, \\ &(\nu_{LT}, \nu_{TT}) = (0.28, 0.33), \\ &(\eta_{LL}, \eta_{TT}) = (30.96, 26.53) \times 10^{-12}\ \text{F/m}, \quad \rho = 1578.0\ \text{kg/m}^3, \end{aligned}$$

$$\begin{aligned} \text{PZT-5A}: &(Y_1, Y_2, Y_3, G_{12}, G_{23}, G_{31}) = (61.0, 61.0, 53.2, 22.6, 21.1, 21.1)\ \text{GPa}, \\ &(\nu_{12}, \nu_{13}, \nu_{23}) = (0.35, 0.38, 0.38), \\ &(d_{31}, d_{32}, d_{33}, d_{15}, d_{24}) = (-171, -171, 374, 584, 584) \times 10^{-12}\ \text{m/V}, \\ &(\eta_{11}, \eta_{22}, \eta_{33}) = (1.53, 1.53, 1.50) \times 10^{-8}\ \text{F/m}, \quad \rho = 7600\ \text{kg/m}^3, \end{aligned}$$

where L and T are directions parallel and transverse to the fibres. Beams with (a) symmetric $[0^\circ/90^\circ/90^\circ/0^\circ]$ and (b) asymmetric $[90^\circ/0^\circ/90^\circ/0^\circ]$ cross-ply substrate, with equal ply thickness, are considered with the orientation given with respect to x-axis and stacking order mentioned from the bottom to the top. Unless specified otherwise, $h_p = 0.1h$. The interface of the PZT layer with the substrate is grounded. The top surface of PZT layer is subjected to either closed circuit condition (C) for which the surface potential $\phi_n^N = \phi_n|_{z=h/2} = \bar{\phi}_n^N$ or open circuit condition (O) for which the applied surface charge density at the top $q_n^N = 0$. Convergence studies have revealed that converged results are obtained by discretizing the electric field across the PZT layer by piecewise linear variation across four equal sublayers.

The accuracy of the present theory is assessed by comparison with the exact piezoelastic solution. Since the number of displacement variables in the present theory is the same as in FSDT, results are also compared with FSDT. No comparison is done with other layerwise theories which involve more displacement unknowns, since the accuracy of the present theory is established directly by comparison with the exact solution.

The frequencies and the modal entities are non-dimensionalized as follows with $S = a/h$, $d_T = 374 \times 10^{-12}$ m/V and $\rho_0 = 1578$ kg/m^3:

$$\bar{\omega} = \omega_n a S_1 (\rho_0 / Y_T)^{1/2}, \quad (\bar{u}, \bar{w}, \bar{\phi}) = (u, w, 10^3 \phi S d_T)/\max(u, w),$$
$$(\bar{\sigma}_x, \bar{\tau}_{zx}) = (\sigma_x, \tau_{zx}) S h / Y_T \max(u, w),$$

where $\max(u, w)$ denotes the largest value of u and w through the thickness for a particular mode and $S_1 = S, 1, 1/S$ for the first three thickness modes, respectively.

Let $\bar{\omega}_{\text{exact}}, \bar{\omega}_{\text{FSDT}}, \bar{\omega}_{\text{present}}$, be the dimensionless natural frequencies predicted by the exact piezoelectric solution, the uncoupled FSDT solution and the present coupled layerwise theory. These natural frequencies for the first three thickness modes for hybrid beams of types a and b for open circuit (O) are compared for $n = 1$ in Table 1 for $S = 5$ (thick beam), 10 (moderately thick beam), 100 (thin beam). The shear correction factor for the FSDT solution is taken as 5/6. It has been noted from the mode shapes that the first, second and third thickness modes primarily relate to flexural, extensional and shear behaviour, respectively. It is observed that the natural frequencies predicted by the present theory are in very good agreement with the exact solution for thin to thick beams with $S \geqslant 5$ for both symmetric and asymmetric substrates. In contrast, FSDT yields far inferior results for the first (flexural) and third (shear) modes in which shear has an influence. While FSDT overestimates the fundamental frequency of beam a with $S = 5$ and 10 by 17.3% and 6.8%, the corresponding errors in the present theory are only 0.5% and 0.25%. For the third mode, the error in FSDT is found to increase for beam a from 19.5% for $S = 5$ to 32.4% for $S = 100$ as the beam becomes thinner. Such a trend is not observed in the present theory for third mode in which, as in the other two modes, the accuracy increases with S for thinner beams with the error for beam a reducing from 7.2% for $S = 5$ to just 0.4% for $S = 100$. The error in the first thickness mode (flexural) frequency ω, for the present theory and FSDT, is plotted versus the thickness ratio h/a in Fig. 1, for spatial modes $n = 1$ and 3 for beam a with open circuit condition. The error increases with h/a and n. The present theory yields quite accurate results for the whole range of h/a whereas the error in FSDT is very much larger, being 23.2% for $n = 3$ for moderately thick beam with $h/a = 0.1$ while the corresponding error in the present theory is only 0.8%.

Table 1
Comparison of natural frequencies of hybrid beams for $n = 1$

Mode	S	Beam a ($h_p/h = 0.1$)			Beam b ($h_p/h = 0.1$)		
		$\bar{\omega}_{\text{exact}}$	$\frac{\bar{\omega}_{\text{FSDT}}}{\bar{\omega}_{\text{exact}}}$	$\frac{\bar{\omega}_{\text{present}}}{\bar{\omega}_{\text{exact}}}$	$\bar{\omega}_{\text{exact}}$	$\frac{\bar{\omega}_{\text{FSDT}}}{\bar{\omega}_{\text{exact}}}$	$\frac{\bar{\omega}_{\text{present}}}{\bar{\omega}_{\text{exact}}}$
1	5	5.5344	1.173	1.005	4.6660	1.131	1.006
	10	7.4425	1.068	1.003	5.7597	1.043	1.003
	100	8.7540	0.996	1.000	6.3634	0.995	1.000
2	5	7.4406	1.024	1.031	7.7328	1.025	1.026
	10	7.8293	1.007	1.009	7.9427	1.005	1.007
	100	8.0159	0.997	1.000	8.0172	0.997	1.000
3	5	2.3379	1.195	1.072	2.1802	1.099	1.036
	10	1.7711	1.245	1.014	1.7878	1.170	1.008
	100	1.4966	1.324	1.004	1.6228	1.220	1.002

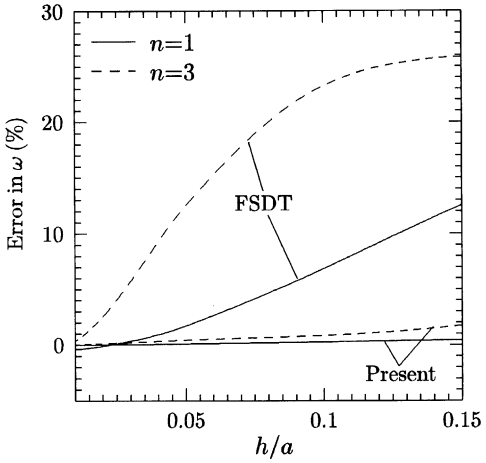

Fig. 1. Error in first thickness mode frequency ω for $n = 1$ and 3 for beam a.

Table 2
Effect of electric boundary conditions on natural frequencies for hybrid beam a for $n = 1$

Mode	S	EBC[a]	$h_p/h = 0.1$		$h_p/h = 0.3$		$h_p/h = 0.5$	
			$\bar{\omega}_{\text{present}}$	$\bar{\omega}_{\text{exact}}$	$\bar{\omega}_{\text{present}}$	$\bar{\omega}_{\text{exact}}$	$\bar{\omega}_{\text{present}}$	$\bar{\omega}_{\text{exact}}$
1	10	O	7.4612	7.4425	5.4673	5.4513	4.5358	4.5220
		C	7.4314	7.4119	5.4047	5.3875	4.4747	4.4608
	100	O	8.7543	8.7540	6.1270	6.1270	4.8468	4.8477
		C	8.7113	8.7110	6.0434	6.0434	4.7692	4.7702
2	10	O	7.8968	7.8293	6.0277	6.0020	5.0517	5.0372
		C	7.8706	7.8031	5.9631	5.9366	4.9614	4.9459
	100	O	8.0166	8.0159	6.2243	6.2240	5.1609	5.1608
		C	7.9945	7.9937	6.1690	6.1688	5.0788	5.0786
3	10	O	1.7962	1.7711	1.8521	1.8292	2.2213	2.1859
		C	1.7954	1.7702	1.8513	1.8283	2.2200	2.1846
	100	O	1.5027	1.4966	1.5904	1.5819	2.0212	1.9836
		C	1.5026	1.4966	1.5904	1.5819	2.0212	1.9836

[a] EBC stands for electric boundary condition.

The effect of electric boundary conditions, namely open circuit (O) or closed circuit (C) with zero potential applied to the top surface of the hybrid beam a, on the natural frequencies is illustrated in Table 2 for $n = 1$. The results obtained from the present theory are compared with the exact solution for the piezolayer thickness ratio $h_p/h = 0.1, 0.3, 0.5$ and span-to-thickness ratio $S = 10, 100$. It is observed that the electric boundary conditions have some influence on the natural frequencies, with the open circuit conditions providing higher frequencies for all cases.

This effect, which is essentially due to piezoelectric coupling, has been captured very well by the present theory. The effect of coupling on the natural frequencies, characterized by the difference between (O) and (C) conditions, increases with h_p/h whereas the effect of S is marginal.

The through-the-thickness distributions of modal displacements $\bar{u}$, $\bar{w}$ and stresses $\bar{\sigma}_x$, $\bar{\tau}_{zx}$ in the fundamental thickness mode (flexural) are shown in Figs. 2–5 for thick and moderately thick beams of types a and b at open circuit condition for $n = 1$. The present results for $\bar{u}$, $\bar{w}$ and $\bar{\sigma}_x$, including the slope discontinuities in u at the layer interfaces, are in excellent agreement with the exact solution for both thick and thin hybrid beams with symmetric and asymmetric substrate laminates. The modal shear stress distribution, obtained by integrating axial equation of motion using the present theory, is also in excellent agreement with the exact solution in all cases. The direct constitutive approach yields the maximum shear stress fairly accurately, but predicts less accurate shear distribution with large errors near the interfaces of the top (piezoelectric) layer and the bottom (composite) layer. In comparison, FSDT has yielded far inferior results for u, $\bar{\sigma}_x$ and

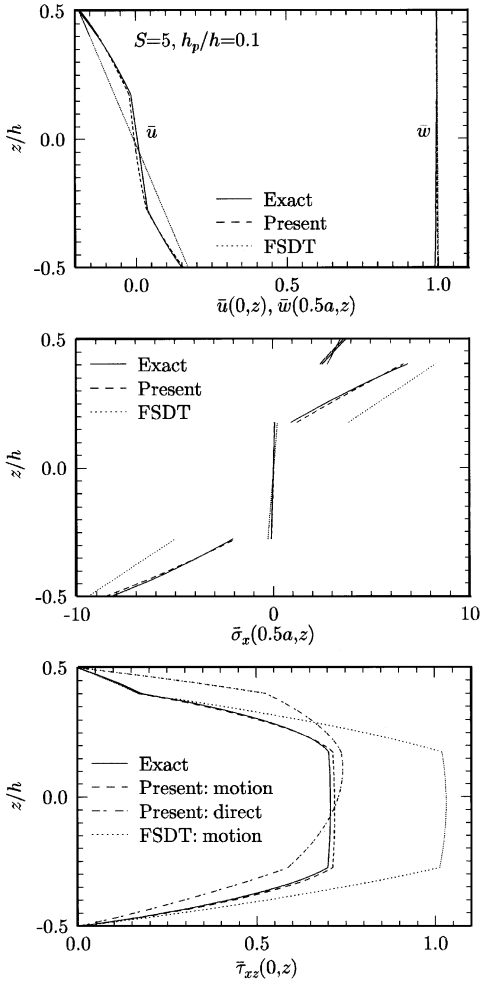

Fig. 2. Through-the-thickness distributions of $\bar{u}$, $\bar{w}$, $\bar{\sigma}_x$, $\bar{\tau}_{zx}$ in the fundamental thickness mode of a thick ($S = 5$) beam a.

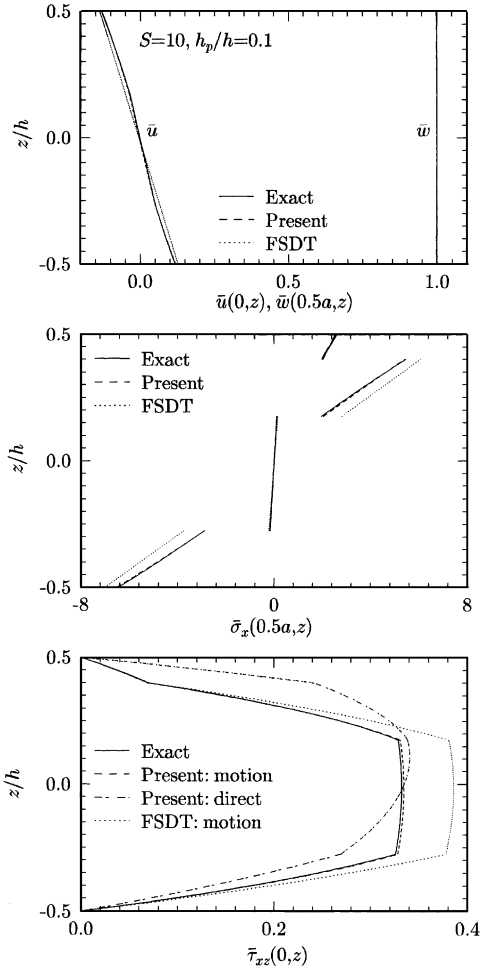

Fig. 3. Through-the-thickness distributions of $\bar{u}$, $\bar{w}$, $\bar{\sigma}_x$, $\bar{\tau}_{zx}$ in the fundamental thickness mode of a moderately thick ($S = 10$) beam a.

postprocessed $\bar{\tau}_{zx}$, the deviations being more pronounced for thicker beams, wherein the simplified kinematic assumptions do not hold well. The errors in maximum $\bar{\tau}_{zx}$ predicted from postprocessing of FSDT results for beams of types a and b with $S = 10$ are 16.1% and 11.0%, respectively, whereas even the direct approach of the present theory yields more accurate results with error reducing to 2.5% and −6.7%, respectively. The distribution of the modal sensory potential across the piezoelectric layer is shown in Fig. 6. It is revealed that the error in the predicted sensory potential is only 1.2% and 0.6% for intermediate thick beams of types a and b, respectively. The error is almost zero (<0.01%) for thin beams with $S = 100$. The distribution of modal potential across the piezoelectric layer at closed circuit condition is shown in Fig. 7 for the hybrid beam of type a for two sets of piecewise linear discretizations over 4 and 8 sublayers. It is seen that the present theory has accurately predicted the maximum potential induced in the piezoelectric layer for both thin and thick beams. The piecewise linear variations of the potential obtained from the present formulation closely follow the exact distribution with excellent matching for 8 sublayers.

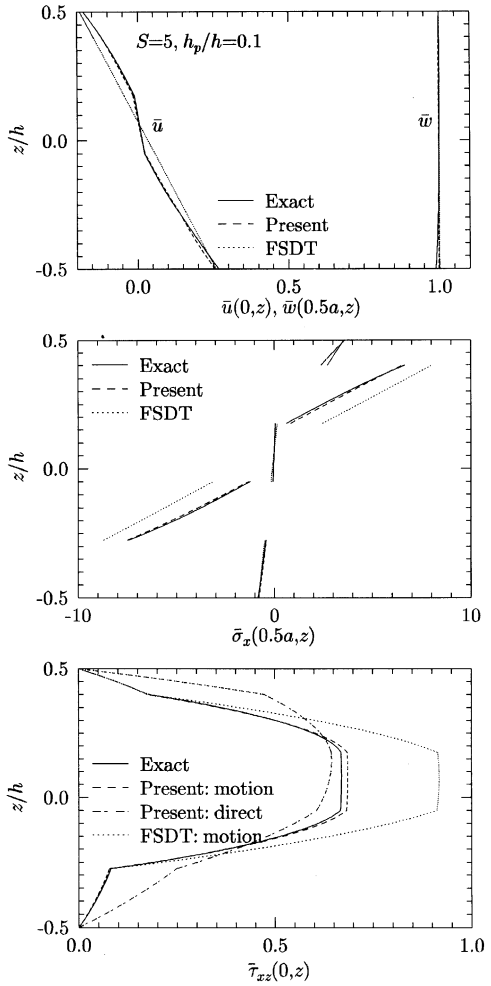

Fig. 4. Through-the-thickness distributions of $\bar{u}$, $\bar{w}$, $\bar{\sigma}_x$, $\bar{\tau}_{zx}$ in the fundamental thickness mode of a thick ($S = 5$) beam b.

The accuracy can be increased either by increasing the number of points across the piezoelectric layer for discretizing the potential or by using higher order interpolation functions Ψ^j.

Consider forced response of beam a with $S = 10$ under sinusoidal harmonic pressure excitation $p_z^2 = p_0 \sin \bar{n}x \cos \Omega t$ on the top surface under closed circuit conditions with actuation potential on the top surface $\phi(x, h/2, t) = \phi^N = \phi_0 \sin \bar{n}x \cos \Omega t$. Let the deflection of the centre of the beam be $w(a/2, 0, t) = w_m \cos \Omega t$ with amplitude w_m. The following non-dimensional variables are used for w_m, ϕ_0 and forcing frequency Ω:

$$\tilde{w}_m = 100 w_m Y_T / h S^4 p_0, \quad \tilde{\phi}_0 = 100 \phi_0 Y_T d_T / h S^2 p_0, \quad \bar{\Omega} = \Omega S a (\rho_0 / Y_T)^{1/2}.$$

The deflection amplitude $\tilde{w}_m$ under harmonic pressure excitation with or without harmonic actuation potential, is presented in Fig. 8 as a function of the forcing frequency $\bar{\Omega}$, for spatial modes $n = 1$ and 3. It is observed that the present theory predicts the harmonic response very accurately for both modes and for both the unactuated and the actuated cases. In contrast, FSDT

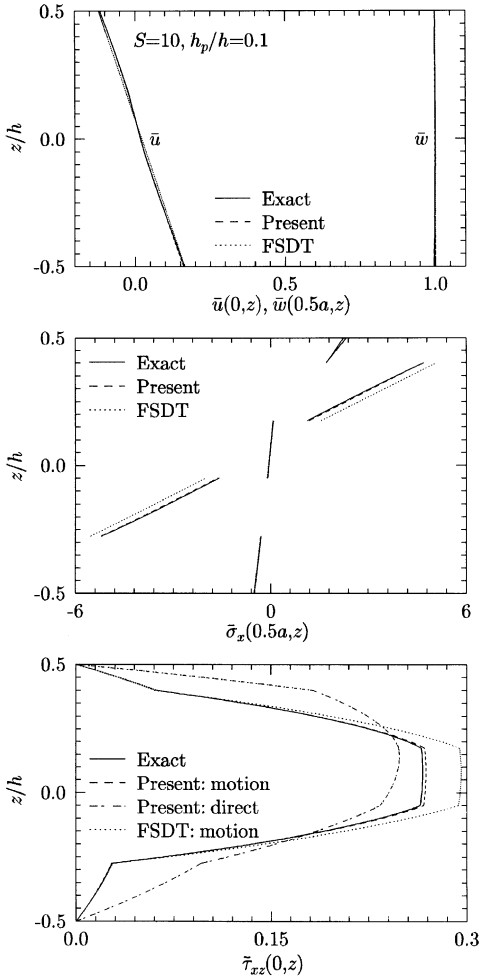

Fig. 5. Through-the-thickness distributions of $\bar{u}$, $\bar{w}$, $\bar{\sigma}_x$, $\bar{\tau}_{zx}$ in the fundamental thickness mode of a moderately thick ($S = 10$) beam b.

results show large error from the exact solution, particularly for the actuation loading case and the error increases for the higher mode with $n = 3$. The large error in $\tilde{w}_m$ in FSDT is primarily due to error of the induced transverse strain due to piezoelectricity from d_{33} coefficient. Similar trend was observed in the statics case using the layerwise theory [23] and the coupled FSDT for rectangular plate [29].

5. Conclusions

A novel coupled electromechanical model has been presented for the dynamic analysis of hybrid beams. The model assumes a third order zig-zag axial displacement field and a piecewise linear electric potential field such that the interlaminar shear stress continuity conditions and shear free conditions on the top and bottom surfaces are satisfied. The accuracy of this theory has

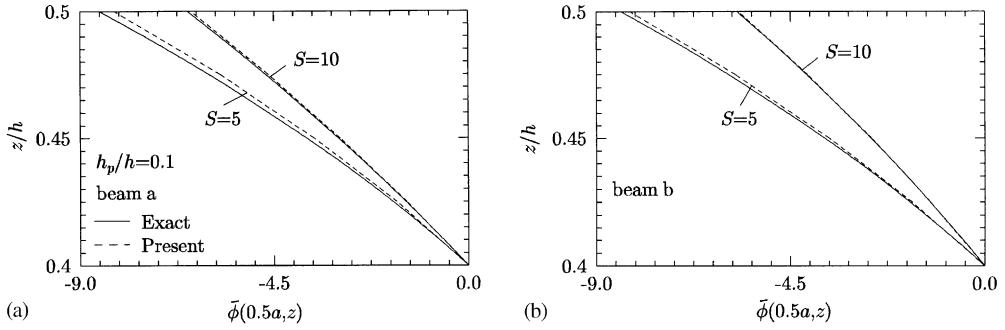

Fig. 6. Open circuit potential across the piezoelectric layer in the fundamental thickness mode of beams a and b.

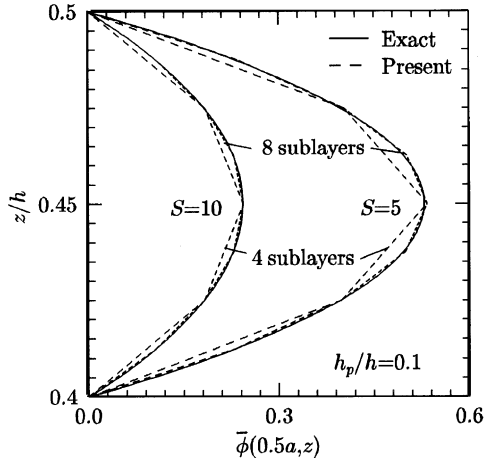

Fig. 7. Closed circuit potential across the piezoelectric layer in the fundamental thickness mode of beam a.

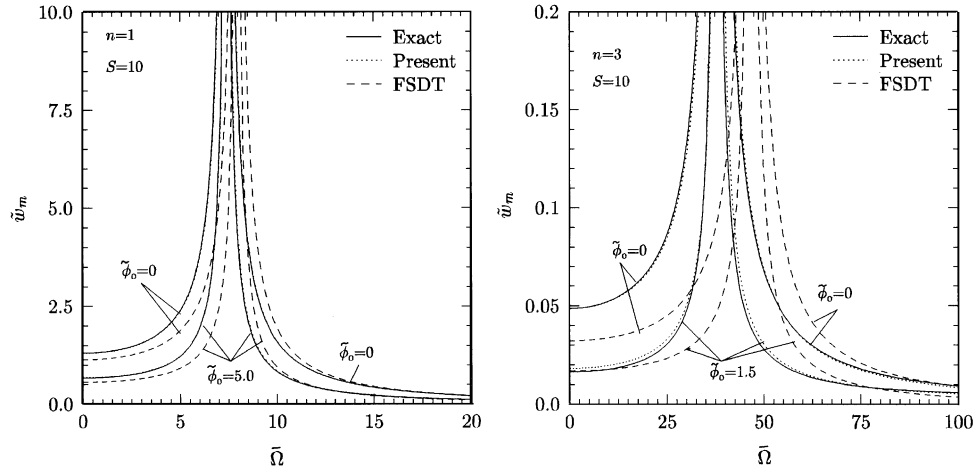

Fig. 8. Maximum mid-surface deflection versus forcing frequency for beam a under harmonic pressure and actuation loading.

been established by comparing the harmonic free and forced vibration response of simply supported hybrid beams with the exact piezoelastic solution. The developed theory yields very good prediction of the natural frequencies and forced response for both thin and thick smart composite beams with symmetric or asymmetric laminate for the substrate. The through-the-thickness variations of the modal displacements, stresses and open as well as closed circuit potential in the piezoelectric layer in the fundamental bending mode are also in excellent agreement with the exact solution for hybrid beams with $S \geqslant 5$.

Comparison of the present results with the uncoupled FSDT solution has established the superiority of the developed model over FSDT. The present theory can effectively model closed circuit as well as open circuit electric boundary conditions in the piezoelectric layer as required in sensory and active applications. Unlike other layerwise theories, the present accurate theory has the advantage of being economical since the number of primary variables for the mechanical field is the same as that of FSDT.

Appendix A. Nomenclature

$A_{11}, B_{11}, D_{11}, F_{11}, G_{11}$	beam stiffness constants
a, b, h	length,width and thickness of the beam
$d_{ij}, e_{ij}; \varepsilon_{ij}, \eta_{ij}$	piezoelectric strain and stress constants; dielectric constants, permittivities
$E_x, E_y, E_z; D_x, D_z; \phi$	electric field components; electric displacements; electric potential
$\bar{E}_{11}^j, \bar{F}_{11}^j, \bar{G}_{11}^j, \bar{H}_{11}^{jl}, D_{55}$	beam stiffness constants
G^j, H^j	electric displacement resultants
$G_{zx}, Y_x; \rho$	shear and Young's moduli; density
I_k, I_k^j, I_k^{jl}	beam inertias
M, K	inertia and stiffness matrices
$N_x, M_x, P_x, S_x^j, \bar{Q}_x^j$	stress resultants
S	thickness parameter a/t
$\bar{U}, P$	displacement and electric potential vector, load vector
$u, w; u_0, w_0$	displacements, midplane displacements
x, y, z	coordinates in axial, width and thickness directions
$\sigma_x, \tau_{zx}; \varepsilon_x, \varepsilon_z, \gamma_{xz}$	stresses; strains
$\Psi^j(z)$	interpolation functions
ω_n, Ω	natural and forcing frequencies
$\beta_k^l, \bar{D}_{55}^j; \beta_5^{jl}, \hat{E}^{jl}$	beam piezoelectric stress constants,beam permittivities
$(*)$	dimensionless entity $(*)$

References

[1] D.A. Saravanos, P.R. Heyliger, Mechanics and computational models for laminated piezoelectric beams, plates and shells, Applied Mechanics Review 52 (1999) 305–320.

[2] P.R. Heyliger, S.B. Brooks, Exact free vibration of piezoelectric laminates in cylindrical bending, International Journal of Solids and Structures 32 (1995) 2945–2960.

[3] P.R. Heyliger, D.A. Saravanos, Exact free vibration of laminated plates with embedded piezoelectric layers, Journal of Acoustical Society of America 98 (1995) 1547–1557.

[4] Z.Q. Cheng, R.C. Batra, Three-dimensional asymptotic analysis of multiple-electroded piezoelectric laminates, American Institute of Aeronautics and Astronautics Journal 38 (2000) 317–324.
[5] S.K. Ha, C. Keilers, F.K. Chang, Three-dimensional finite element analysis of composite structures containing distributed piezoceramic sensors and actuators, American Institute of Aeronautics and Astronautics Journal 30 (1992) 772–780.
[6] T. Bailey, J.E. Hubbard, Distributed piezoelectric-polymer active vibration control of a cantilever beam, Journal of Guidance, Control and Dynamics 8 (1985) 605–611.
[7] S. Im, S.N. Atluri, Effects of a piezo-actuator on a finitely deformed beam subject to general loading, American Institute of Aeronautics and Astronautics Journal 27 (1989) 1801–1807.
[8] R. Chandra, I. Chopra, Structural modelling of composite beams with induced-strain actuators, American Institute of Aeronautics and Astronautics Journal 31 (1993) 1692–1701.
[9] D.H. Robbins, J.N. Reddy, Analysis of piezoelectrically actuated beams using a layer-wise displacement theory, Computers and Structures 41 (1991) 265–279.
[10] H.S. Tzou, Distributed sensing and controls of flexible plates and shells using distributed piezoelectric element, Journal of Wave Material Interaction 4 (1989) 11–29.
[11] C.K. Lee, Theory of laminated piezoelectric plates for the design of distributed sensors/actuators. Part 1: governing equations and reciprocal relationships, Journal of Acoustical Society of America 87 (1990) 1144–1158.
[12] E.F. Crawley, K.B. Lazarus, Induced strain actuation of isotropic and anisotropic plates, American Institute of Aeronautics and Astronautics Journal 29 (1991) 944–951.
[13] K. Chandrashekhara, A.N. Agarwal, Active vibration control of laminated composite plates using piezoelectric devices: a finite element approach, Journal of Intelligent Materials Systems & Structures 4 (1993) 496–508.
[14] P.F. Pai, A.H. Nayfeh, K. Oh, D.T. Mook, A refined nonlinear model of composite plates with integrated piezoelectric actuators and sensors, International Journal of Solids and Structures 30 (1993) 1603–1630.
[15] K. Chandrashekhara, P. Donthireddy, Vibration suppression of composite beams with piezoelectric devices using a higher order theory, European Journal of Mechanics A/Solids 16 (1997) 709–721.
[16] X.Q. Peng, K.Y. Lam, G.R. Liu, Active vibration control of composite beams with piezoelectrics: a finite element model with third order theory, Journal of Sound and Vibration 209 (1998) 635–650.
[17] J.H. Huang, T.L. Wu, Analysis of hybrid multilayered piezoelectric plates, International Journal of Engineering Science 34 (1996) 171–181.
[18] D. Huang, B. Sun, Approximate analytical solutions of smart composite Mindlin beams, Journal of Sound and Vibration 244 (2001) 379–394.
[19] J.A. Mitchell, J.N. Reddy, A refined hybrid plate theory for composite laminates with piezoelectric laminae, International Journal of Solids and Structures 32 (1995) 2345–2367.
[20] X. Zhou, A. Chattopadhyay, H. Gu, Dynamic responses of smart composite using a coupled thermo-piezoelectric-mechanical model, American Institute of Aeronautics and Astronautics Journal 38 (2000) 1939–1948.
[21] D.A. Saravanos, P.R. Heyliger, Coupled layerwise analysis of composite beams with embedded piezoelectric sensors and actuators, Journal of Intelligent Materials Systems & Structures 6 (1995) 350–363.
[22] D.A. Saravanos, P.R. Heyliger, Layerwise mechanics and finite element for the dynamic analysis of piezoelectric composite plates, International Journal of Solids and Structures 34 (1997) 359–378.
[23] S. Kapuria, An efficient coupled theory for multi-layered beams with embedded piezoelectric sensory and active layers, International Journal of Solids and Structures 38 (2001) 9179–9199.
[24] M. Cho, R.R. Parmerter, Efficient higher order composite plate theory for general lamination configurations, American Institute of Aeronautics and Astronautics Journal 31 (1993) 1299–1306.
[25] X. Shu, L. Sun, An improved simple higher-order theory for laminated composite plates, Computers and Structures 50 (1994) 231–236.
[26] B.A. Auld, in: Acoustic Fields and Waves in Solids, Vol. I, Wiley, New York, 1973.
[27] H.F. Tiersten, Linear Piezoelectric Plate Vibrations, Plenum, New York, 1969.
[28] K. Xu, A.K. Noor, Y.Y. Tang, Three-dimensional solutions for coupled thermoelectroelastic response of multilayered plates, Computer Methods in Applied Mechanics and Engineering 126 (1995) 355–371.
[29] S. Kapuria, P.C. Dumir, Coupled FSDT for piezothermoelastic hybrid rectangular plate, International Journal of Solids and Structures 37 (2000) 6131–6153.